Contribution of electronic structure to the large thermoelectric power in layered cobalt oxides

Tsunehiro Takeuchi
Research Center for Advanced Waste and Emission Management, Nagoya University, Nagoya 464-8603, Japan

Takeshi Kondo, Tsuyoshi Takami, Hirofumi Takahashi, Hiroshi Ikuta, Uichiro Mizutani, and Kazuo Soda
Department of Crystalline Materials Science, Nagoya University, Nagoya 464-8603, Japan

Ryoji Funahashi, Masahiro Shikano, and Masashi Mikami
National Institute of Advanced Industrial Science and Technology Kansai, Ikeda 563-8577, Japan

Syunsuke Tsuda, Takayoshi Yokoya, and Shik Shin
Institute of Solid State Physics, University of Tokyo, Kashiwa 277-8581, Japan

Takayuki Muro
Japan Synchrotron Radiation Research Institute, Hyogo 679-5198, Japan

(Received 1 October 2003; revised manuscript received 14 November 2003; published 19 March 2004)

With a strong help of high-resolution photoemission spectroscopy we demonstrate in this paper that the large thermoelectric power observed in the layered cobalt oxides, such as $Ca_3Co_4O_9$, $Na_{0.6}CoO_2$, and $Bi_2Sr_2Co_2O_9$, can be well accounted for with the Boltzmann-type metallic electrical conduction. An intense peak with 1.5–2 eV in width was observed in the photoemission spectra with its center at 1.0 eV below the Fermi level E_F in these compounds. The density of states at E_F is finite but negligibly small at room temperature, because E_F is located near the high-energy edge of this narrow band. We calculated thermoelectric power S using the Boltzmann transport equation with the electronic structure near E_F determined by the photoemission measurement. The calculated S shows fairly good consistency with the measured value both in its magnitude and the temperature dependence.

DOI: 10.1103/PhysRevB.69.125410 PACS number(s): 72.15.Jf, 71.20.Be

I. INTRODUCTION

Layered cobalt oxides characterized by two-dimensionally spanned CoO_2 triangular-lattice consisting of edge-shared CoO_6 octahedrons have attracted a great deal of interest because of their possession of unusual electrical properties, such as superconductivity in water intercalated $Na_{0.35}CoO_2$,[1] coherent-incoherent transition with varying temperature in $Bi_2Pb_2Co_2O_9$,[2] and a large thermoelectric power with metallic electrical conduction observed for $NaCoO_2$, $Bi_2Sr_2Co_2O_9$, $Ca_3Co_4O_9$ $[(Ca_2CoO_3)_xCoO_2, x \approx 0.62]$, and $Tl_{0.4}(Sr_{0.9}O)_{1.12}CoO_2$.[3–9] The large thermoelectric power and the metallic electrical conduction are especially important from the technological point of view because the large thermoelectric power S and the large electrical conductivity σ together with a low thermal conductivity κ are necessary for the development of a practical thermoelectric material that has been regarded as one of the key technologies of energy saving and environmental protection.

Thermoelectric power as well as the electrical conductivity varies as a function of carrier concentration. These two quantities, in general, have opposite behavior in their carrier-concentration dependence; thermoelectric power increases while electrical conductivity decreases with decreasing carrier concentration.[10] It has been widely believed, therefore, that there is an optimal carrier concentration of about 10^{19} cm^{-3} that provides the largest thermoelectrical figure of merit $Z=(S^2\sigma)/\kappa$. In this respect, doped semiconductors have been frequently employed as thermoelectric devices and their performance has been discussed in terms of the carrier concentration.[10]

Thermoelectric power in Na_xCoO_2 was reported to exceed 80 μV/K at room temperature, even though its electrical resistivity is lower than 200 $\mu\Omega$ cm at room temperature.[3,4] Other layered cobalt oxides also possess a large thermoelectric power exceeding 100 μV/K at room temperature while maintaining metallic electrical resistivity less than 10 mΩ cm.[5–9] This is surprising because two contradicting conditions, large thermoelectric power and small electrical resistivity, are simultaneously achieved in these materials. In addition, these cobalt oxides show rather low thermal conductivity due most likely to the misfit structure between the CoO_2 layers and other layers, such as rocksalt layers (Ca_2CoO_3 layers) in $Ca_3Co_4O_9$ and Na layers in Na_xCoO_2.[11] A combination of a large thermoelectric power, a large electrical conductivity, and a small thermal conductivity produces a large dimensionless figure of merit $ZT=0.87$ at 973 K in $Ca_3Co_4O_9$.[9] Thus these layered cobalt oxides have been regarded as one of the most promising candidates for the practical thermoelectric material. Their high-temperature stability is another advantage, particularly for the use at high temperatures, which further prompted us to utilize the cobalt oxides as a thermoelectric device at high temperatures.

Koshibae *et al.* proposed a theory to account for the pos-

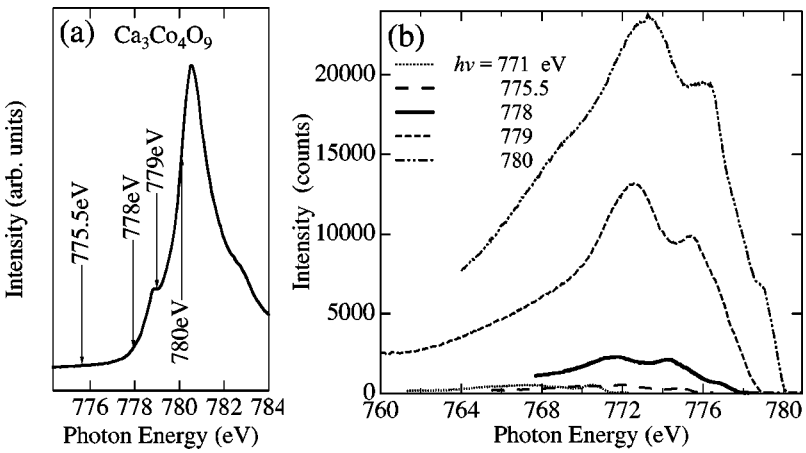

FIG. 1. (a) Co $2p$-$3d$ x-ray-absorption spectrum of $Ca_3Co_4O_9$ measured at 20 K. (b) X-ray photoemission spectroscopy (XPS) spectra measured with various incident photon energies from $h\nu = 771$ eV to 780 eV at 20 K. Co $2p$-$3d$ resonance takes place at energies larger than $h\nu = 775.5$ eV.

session of the large thermoelectric power in cobalt oxides on the basis of the Heikes formula.[12,13] In their theory, Co $3d$ electrons are not considered to have extended Bloch states but to be rather localized, and degeneracy in the cobalt $3d$ states plays an important role in enhancing the thermoelectric power due to their large configurational entropy. Though their theory has been frequently employed to interpret the experimentally observed large thermoelectric power,[8,14–16] the metallic electrical conduction always reminds us of the need to consider that the Boltzmann-type electrical conduction with extended Bloch states takes place in these layered cobalt oxides, and that the electronic structure specific to the two-dimensional CoO_2 triangular-lattice layer contributes to a large thermoelectric power under the Boltzmann-type electron-transport mechanism. Notably Singh predicted on the basis of the LDA-LAPW calculation that the large thermoelectric power of 110 μV/K at 300 K can be reproduced from the metallic electronic structure.[17]

In the present study, electronic structure in the γ-phase $Na_{0.6}CoO_2$ (abbreviated as γ-NCO),[18] $Bi_2Sr_2Co_2O_9$ (abbreviated as BSCO), and $Ca_3Co_4O_9$ (abbreviated as CCO) is investigated in detail using high-resolution ultraviolet photoemission spectroscopy (UPS) and Co $2p$-$3d$ resonant photoemission spectroscopy (RPES). The electron-transport properties of both electrical conductivity and thermoelectric power for these layered cobalt oxides and their sample dependence are discussed in terms of the measured electronic structure near the Fermi level E_F, and the specific electronic structure responsible for the metallic electrical conduction and the large thermoelectric power is experimentally investigated. The temperature dependence of the thermoelectric power $S(T)$ was calculated from the measured electronic structure within the context of the Boltzmann transport equation. We demonstrate that the large thermoelectric power in the layered cobalt oxides can be well accounted for in terms of the Boltzmann-type metallic conduction in a narrow band specific to the two-dimensional CoO_2 layers.

II. EXPERIMENTAL PROCEDURE

High-quality single crystals were grown by the flux method. The details of the sample preparation were reported elsewhere.[9,19,20] Bulk-sensitive Co $2p$-$3d$ RPES measurements with incident photon energies of $h\nu = 775$–780 eV were performed in the beam line BL25SU at the third generation 8 GeV synchrotron radiation facility SPring-8, Hyogo, Japan. The energy resolution of the RPES measurements was better than 120 meV, which was defined as the energy width of the intensity reduction from 90% to 10% at the Fermi edge of the reference gold electrically contacting with the measured samples.

In order to investigate the electronic structure near E_F in detail, HeIα UPS measurements with 20 meV energy resolution were also performed at the Institute for Solid State Physics, The University of Tokyo. We used Gammadata-Scienta SES2002 hemispherical analyzer in both RPES and UPS measurements. The clean surfaces were obtained by cleaving samples under the ultrahigh vacuum condition with a base pressure better than 1×10^{-10} Torr. No significant angle dependence was observed in both RPES and UPS measurements most likely because the cleaved surfaces have some roughness, which is large enough to smear the angle dependence of the photoelectron intensity.

III. RESULTS

The Co $2p$-$3d$ x-ray-absorption spectroscopy (XAS) data of the CCO measured at 20 K is shown in Fig. 1(a). Valence-band photoemission signals were accumulated at 20 K using different photon energies, which are marked with arrows on the XAS spectrum in Fig. 1(a). The resulting photoemission spectra are shown in Fig. 1(b). The Co $2p$-$3d$ resonance takes place at the incident energies $h\nu \geqslant 775$ eV. We employed a slightly lower incident energy of $h\nu = 778$ eV than the one providing the maximum intensity ($h\nu = 780$ eV) for the Co $2p$-$3d$ on-resonant measurements to avoid an influence of undesirable Auger process. The photoemission intensity even at $h\nu = 778$ eV is enhanced almost ten times larger than that in the off-resonant one at $h\nu = 771$ eV.

Figures 2(a) and 2(b) show the Co $2p$-$3d$ on-resonant and off-resonant photoemission spectra accumulated at $h\nu = 778$ eV and 771 eV, respectively. The off-resonant spectra of all these compounds exhibit an intense peak at $\sim$1.0 eV below E_F. We consider that the electronic states causing this intense peak are closely related with their possession both of the large thermoelectric power and metallic conduction, be-

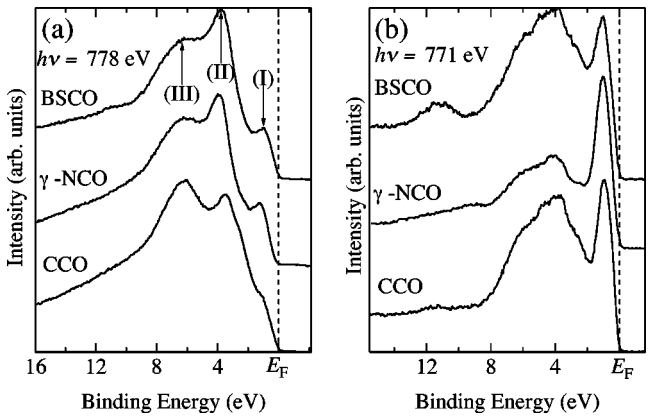

FIG. 2. (a) Co $2p$-$3d$ on-resonant spectra of $Ca_3Co_4O_9$ (CCO), $Bi_2Sr_2Co_2O_9$ (BSCO), and γ-$Na_{0.6}CoO_2$ (γ-NCO) measured with an incident energy of $h\nu = 778$ eV at 20 K. Three humps marked with (I), (II), and (III) are observed in all spectra at 1 eV, 3.9 eV, and 6.5 eV, respectively. (b) Off-resonant XPS spectra of CCO, γ-NCO, and BSCO measured at 20 K. All spectra are characterized by an intense peak centered at $\sim$1 eV. The Fermi level is located near the high-energy edge of this peak.

cause E_F is located near the high-energy end of this peak. However, this peak turned out to be less obvious in the on-resonant spectra, though the intensity itself was increased more than five times larger due to the Co $2p$-$3d$ resonance. This means, thereby, that the band(s) lying in the energy range from E_F to 2.0 eV below E_F consists both of the O $2p$ and Co $3d$ components, and is dominated more by O $2p$ component than by the Co $3d$ component. On the basis of the LAPW-LDA band calculation, Singh reported that the Co $3d$-O $2p$ hybridization is weak in the NCO and the bands crossing the E_F were assigned as the Co $3d$ bands.[17] Our observation is certainly inconsistent with his LAPW-LDA band calculation. Recently, however, Asahi *et al.* calculated the band structure of CCO by FLAPW method on the basis of precisely determined atomic structure, and they predicted a presence of strong hybridization between Co $3d$ and O $2p$.[21] In their report, the bands near E_F consist of Co $3d$-O $2p$ antibonding bands, and this accounts very well for our present observations.

The on-resonant spectra of the BSCO show similarity with that of the γ-NCO. Only the cobalt $3d$ component is strongly enhanced in the RPES spectra and cobalt atoms exist only in a site of the CoO_2 layer both in the BSCO and γ-NCO. Therefore, it is natural to assume that the RPES spectra only reflect the electronic structure in the CoO_2 layer. The similarity in the RPES spectra between the γ-NCO and BSCO indicates that the electronic structure in the CoO_2 layer in both compounds is not greatly affected by the adjacent layers unique to the respective ones.

Three humps are clearly observed at energies marked with (I) at $E = 1.0$, (II) at $E = 3.9$, and (III) at $E = 6.5$ eV in the on-resonant spectra of the BSCO and γ-NCO. Those humps are assigned as the bonding e_g, bonding t_{2g}, and antibonding t_{2g} bands from the cluster levels for the CoO_6 tetrahedron, as schematically illustrated in Figs. 3(a)–3(c). The width of the e_g bands is naturally considered to be wider than that of the t_{2g} bands because of their larger transfer integral. The hump spreading over a wide energy range of 3–8 eV can be safely assigned as the bonding e_g bands.

The on-resonant RPES spectrum in the CCO is fairly different from those in the other compounds. This difference in the spectrum shape must be attributed to its possession of an extra cobalt site in the rocksalt (Ca_2CoO_3) layer.[11] Since CCO has the same CoO_2 layer as that in the BSCO and γ-NCO and no significant difference in the electronic structure of the CoO_2 layer was observed between BSCO and γ-NCO, we assume here that the CoO_2 layer in the CCO also has essentially the same electronic structure as that in the NCO and BSCO.

On the basis of this assumption, we deduced the cobalt $3d$ partial density of states in the rocksalt layer by subtracting the γ-NCO's Co $2p$-$3d$ on-resonant spectrum from the CCO's on-resonant spectrum. In this analysis, the energy of the γ-NCO was shifted by 140 meV to higher energy so that the peaks at 1 eV in both spectra coincide with each other. The spectrum intensity was normalized such that the ratio of the integrated intensity of CCO to that of γ-NCO should be equal to the ratio of Co atoms in all layers to those belonging to the CoO_2 layer, i.e., 10 to 6.[11]

The spectrum deduced for the rocksalt layer in CCO is shown in Fig. 4. Three structures are clearly observed: a

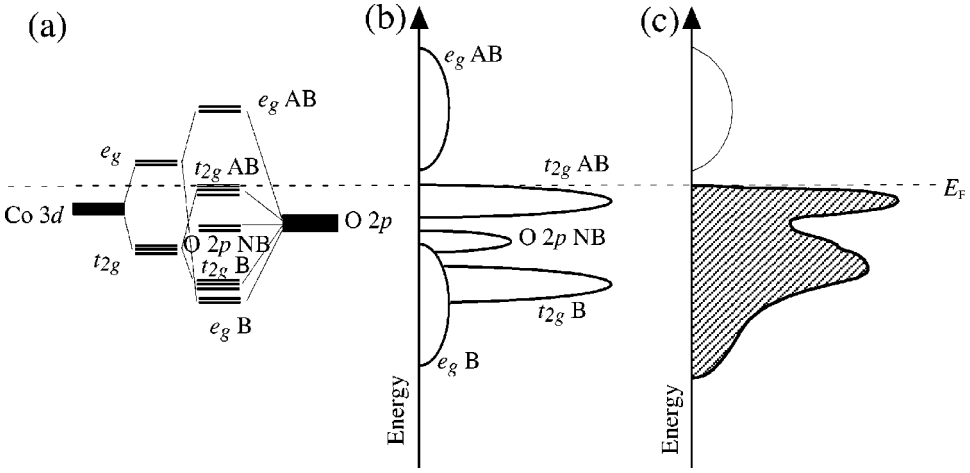

FIG. 3. Schematic illustration of (a) cluster levels in the CoO_6 octahedron, (b) the density of states in the network of the CoO_6 octahedrons, and (c) XPS spectrum expected to be observed for the network of the CoO_6 octahedrons.

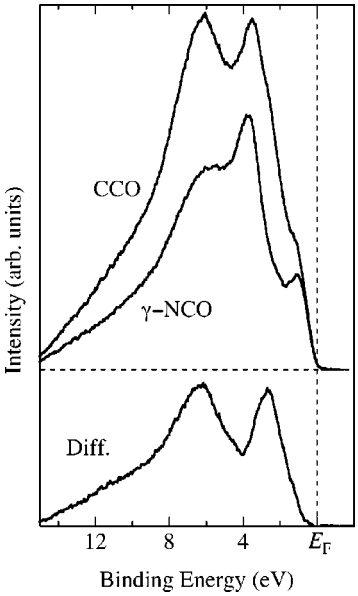

FIG. 4. Co $2p$-$3d$ on-resonant spectra of $Ca_3Co_4O_9$ (CCO) and γ-$Na_{0.6}CoO_2$ after subtracting the background intensity. The spectrum of the γ-NCO was shifted by 240 meV towards higher binding energy, and its intensity was normalized such that the integrated intensity becomes 60% of that of the CCO. By considering NCO's spectrum as that of the CoO_2 layer in the CCO and subtracting it from that of CCO, we obtained a spectrum representing the rocksalt layer in the CCO.

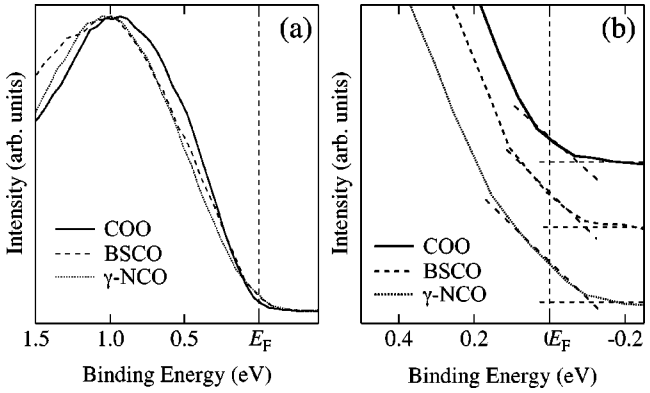

FIG. 5. (a) Off-resonant photoemission spectra of $Ca_3Co_4O_9$ (CCO), $Bi_2Sr_2Co_2O_9$ (BSCO), and γ-$Na_{0.6}CoO_2$ measured at 20 K. The leading edge of the 1 eV peak of CCO shows lowest binding-energy, while that of the γ-NCO stays at the highest. The spectra in the vicinity of E_F are enlarged in (b). Spectra of CCO and BSCO are vertically shifted to clearly distinguish each spectrum. Horizontal dashed lines indicate background intensity at E_F. A finite intensity persists at E_F in all compounds. All spectra show common slope at E_F that would be caused by the energy resolution of the measurement (see slopes with thin dashed lines as a guide to eye). Though its leading edge stays in the lowest binding-energy, the intensity at E_F in CCO shows much smaller value than that in the others. This shows good consistency with the highest electrical resistivity of CCO among these three cobalt oxides.

sharp peak at 2.4 eV, a slightly broad one centered at 6.4 eV, and a broad hump extending up to 12 eV. The symmetry about the cobalt atom in the rocksalt layer gives rise to the t_{2g} and e_g bands in the same way as those in the CoO_2 layers. The sharp peak at $\sim$2.4 eV is assigned as the antibonding t_{2g} bands and the peak at 6.4 eV mainly as the bonding t_{2g} bands. Widely extended bands over the energy range $3<E<12$ eV is regarded as the bonding e_g bands. Obviously the valence band in the rocksalt layer hardly reaches the Fermi level. This result suggests that the metallic electrical conduction in CCO arises only from the CoO_2 layer rather than from the rocksalt layer.

The deduced Co $3d$ partial density of states in the rocksalt layer shows good consistency with the FLAPW bands calculated by Asahi *et al.*[21] in the point that the e_g bands are spread over a wide energy range and the antibonding t_{2g} bands and bonding t_{2g} bands lie at 2 and 6 eV, respectively. However, their calculation shows that the widely spread e_g bands in the rocksalt layer lies across E_F while the Co $3d$ partial density of states in our present analysis shows no intensity at E_F. Since the widely extended e_g bands in the FLAPW calculation provide only a very small density of states at E_F, our rough assumption of the common electronic structure in the CoO_2 layer among CCO, BSCO, and γ-NCO might cause this inconsistency. Although absence of the widely extended e_g bands at E_F cannot be unambiguously proved, we decided to employ the electronic structure with no e_g bands near E_F in our analysis of thermoelectric power performed in the Discussion.

Co $2p$-$3d$ RPES spectra for BSCO, γ-NCO, and CCO suggest that the valence band in an energy range from E_F to 1 eV is dominated by the electronic structure in the CoO_2 layer. It is, therefore, very important to compare the energy of the spectrum edge near E_F in the RPES spectra for these three compounds, because it reflects the carrier concentration in the CoO_2 layer. As shown in Fig. 5(a), the high-energy edge in the off-resonant spectrum of the CCO is located at the highest binding energy and that in the γ-NCO shows the lowest. This tendency is also confirmed with the energy of peak (II) in the on-resonant spectra; those are observed at 3.9, 3.85, and 3.55 eV for the γ-NCO, BSCO, and CCO, respectively. These results suggest that the hole concentration in the CoO_2 layer increases in the sequence of γ-NCO, BSCO, and CCO.

The Fermi level E_F is located at the high-energy edge of the peak centered at about 1.0 eV in the off-resonant spectra for these three cobalt oxides. The metallic electrical conduction commonly observed in these layered cobalt oxides can be taken as the evidence for the possession of a finite density of states at E_F. We found that the off-resonant spectra of these three compounds shown in Fig. 5(b) possess a common slope at E_F, which would reflect the presence of Fermi edge broadened by the energy resolution of the measurement.

In order to unambiguously confirm the presence of the Fermi edge in these layered cobalt oxides, we employed UPS measurements of an energy resolution better than 20 meV. Figures 6(a)–6(c) show the UPS spectra of the CCO, BSCO, and γ-NCO, respectively, measured with monochromated HeIα at various temperatures. We observed that the density of states at the Fermi level shows a finite value at room temperature in all compounds, though the Fermi edge was

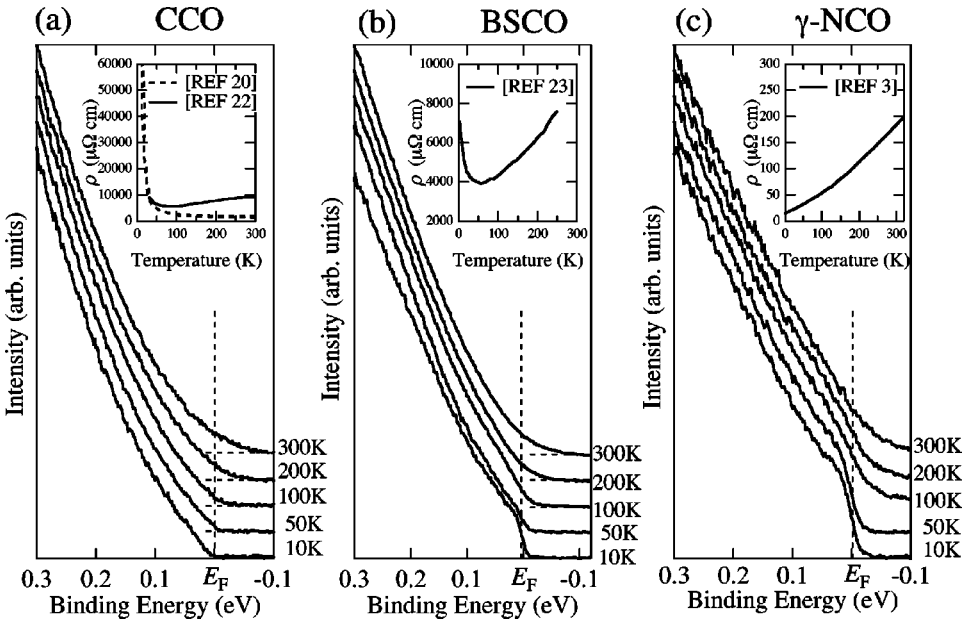

FIG. 6. UPS spectra near E_F measured at 10, 59, 100, 200, and 300 K for (a) $Ca_3Co_4O_9$, (b) $Bi_2Sr_2Co_2O_9$, and (c) γ-$Na_{0.6}CoO_2$. The temperature dependence of electrical resistivity of each compound is shown in the insets.

not clearly observed because of the large thermal broadening at room temperature. The Fermi edge in the UPS spectrum of the BSCO and γ-NCO, however, becomes evident with decreasing temperature. On the other hand, the UPS spectrum of the CCO possesses no clear Fermi edge even in low temperatures below 100 K. We found that the electrical resistivity in these cobalt oxides can be well accounted for by the observed UPS spectrum. This will be discussed in the Discussion.

IV. DISCUSSION

A. Electrical resistivity

The electrical resistivity reported for these compounds are shown in the insets of Figs. 6(a)–6(c).[3,20,22,23] All compounds show a metallic electrical resistivity less than 10 m Ω cm at room temperature with a positive temperature coefficient, which is a typical behavior of the Boltzmann-type electrical conduction. One may notice that the observed UPS intensity near the Fermi edge is well consistent with the behavior of the electrical resistivity; electrical resistivity in the CCO rapidly increases below 100 K and apparently diverges at zero temperature,[23] while the other two compounds exhibit a finite residual resistivity less than 8 m Ω cm.[3,9] The smallest electrical resistivity observed for the γ-NCO is also consistent with the possession of the largest intensity at the Fermi level among these three cobalt oxides.

It is very important to note that the Hall coefficient of the CCO shows a large enhancement in its magnitude as well as its electrical resistivity below 100 K.[7] The increase in the Hall coefficient and electrical resistivity at low temperatures in the CCO strongly indicates that the density of states at E_F gradually decreases with decreasing temperature below 100 K, and that an energy gap eventually opens across E_F at a temperature below 50 K. The density of states at E_F was indeed absent in the UPS spectra of CCO at 10 K, and the gap width in the CCO is estimated to be less than 20 meV at 10 K. We strongly expect that the increase in the electrical resistivity with decreasing temperature in the CCO cannot be fitted to an exponential-type equation to describe the thermal excitation of electrons across a rigid band gap, because the energy gap we observed in the UPS spectra is strongly temperature dependent.

Though an increase in the electrical resistivity with decreasing temperature was also observed for the BSCO below 50 K, as shown in the inset of Fig. 6(b), a finite residual resistivity and a clear Fermi edge in the UPS spectrum indicate that the Boltzmann-type metallic conduction would persist in the BSCO down to the lowest temperature. Although the origin for the increase in the electrical resistivity at low temperatures in the BSCO is not well understood, we expect that it would be caused by the reduction of the density of states with decreasing temperature in the same way as in the CCO.

Scaling theory[24] suggested that the conduction electrons in one- or two-dimensional systems are more easily localized than those in the three-dimensional systems. All samples we employed in this study actually have strong anisotropy in the structure and properties. Besides, the BSCO and CCO are known to have misfit between layers that must cause random potential scattering of conduction electrons. It is possible to consider, therefore, that the carrier localization due to the multiple elastic scattering is another candidate for the factors of the increase in the electrical resistivity of CCO and BSCO with decreasing temperature below 50 K. Precise determination of the temperature dependence of the electrical resistivity $[\rho(T)]$ is required to reveal whether carrier localization takes place in these cobalt oxides. Since we have only limited information about $\rho(T)$, we decided to leave this carrier localization problem without discussing in more detail.

Before ending this section, we should briefly comment on the origin of the energy-gap and -pseudogap formation observed in the CCO. Two possible mechanisms are considered for the energy-gap development. Nesting of the Fermi sur-

face is one of the candidates, because the spin-density wave (SDW) would be naturally caused by an energy gain associated with a gap formation across E_F as a consequence of a nesting of the Fermi surface(s). The formation of SDW was indeed observed by the muon spin-resonance measurement for layered cobalt oxides.[22] The strong electron correlation, that is, the second candidate, has been also discussed in relation to the gap development. Theoretical studies on a triangular lattice in the presence of the strong correlation predicted the development of an energy gap across E_F.[25–27] Notably, a development of the SDW without the nesting of the Fermi surface(s) was also predicted in their studies. We are now in progress with angle-resolved photoemission spectroscopy (ARPES) measurements on these cobalt oxides, and the presence or the absence of the nesting will be clearly confirmed by the ARPES measurement.

B. Thermoelectric power

In this section, we concentrate on calculating the temperature dependence of the thermoelectric power within the Boltzmann transport mechanism by analyzing the electronic structure near the Fermi level deduced from the present UPS measurements.

Thermoelectric power is expressed by using the formula as

$$S(T)=\frac{1}{eT}\frac{\int_{-\infty}^{\infty}\sigma(\varepsilon)(\varepsilon-\mu)\frac{\partial f(\varepsilon)}{\partial\varepsilon}d\varepsilon}{\int_{-\infty}^{\infty}\sigma(\varepsilon)\frac{\partial f(\varepsilon)}{\partial\varepsilon}d\varepsilon}, \tag{1}$$

where $\sigma(\varepsilon)$ represents the electrical conductivity at the energy ε.[28,29] The numerator provides the total energy flow carried by the conduction electrons, and the denominator simply provides electrical conductivity multiplied by temperature and the charge of an electron. The product of the thermoelectric power and temperature can be, therefore, understood as a mean energy flow carried by a conduction electron. Note here that even though the integration in Eq. (1) is calculated over a whole energy range, the energy derivative of the Fermi-Dirac distribution function $\partial f(\varepsilon)/\partial\varepsilon$ plays as a very narrow energy-window function, so that it allows us to ignore the integration in energy ranges more than a few k_BT above and below E_F.

If the temperature is low enough to use the condition of $\partial f(\varepsilon)/\partial\varepsilon=\delta(\varepsilon=E_F)$, Eq. (1) turns out to be the frequently employed formula of

$$S(T)=\frac{\pi^2 k_B T}{3e}\left[\frac{\partial \ln\sigma(\varepsilon)}{\partial\varepsilon}\right]_{\varepsilon=E_F}. \tag{2}$$

Although Eq. (2) is commonly employed in many textbooks, it does not provide the real temperature dependence especially when $\sigma(\varepsilon)$ varies within an energy range of a few k_BT centered at E_F. The layered cobalt oxide we study in this paper is a typical case with $\sigma(\varepsilon)$ possessing a strong energy dependence.

By assuming (a) the Boltzmann-type metallic conduction in a two-dimensional isotropic band, (b) an energy-independent group velocity v_G, and (c) an energy-independent relaxation time τ in a narrow energy range where $\partial f(\varepsilon)/\partial\varepsilon$ has finite value, Eq. (1) is now rewritten as

$$S(T)=\frac{1}{eT}\frac{\int_{-\infty}^{\infty}N(\varepsilon)(\varepsilon-\mu)\frac{\partial f(\varepsilon)}{\partial\varepsilon}d\varepsilon}{\int_{-\infty}^{\infty}N(\varepsilon)\frac{\partial f(\varepsilon)}{\partial\varepsilon}d\varepsilon}, \tag{3}$$

where $N(\varepsilon)$ is the density of states at the energy ε. As mentioned above, information about $N(\varepsilon)$ is needed only within a narrow energy range of a few k_BT in width centered at E_F because of the presence of $\partial f(\varepsilon)/\partial\varepsilon$ in the integrand. Note here that the density of states of our interest can be deduced from the measured UPS spectrum at room temperature by dividing it by the Fermi-Dirac distribution function. It is also worthwhile to mention that the measured UPS intensity is not equal to the density of states but is proportional to it. Fortunately, $N(\varepsilon)$ appears in both numerator and denominator, so that the proportional constant is canceled upon the insertion of the measured UPS intensity. It is also important to recognize upon substitution of the UPS intensity for $N(\varepsilon)$ that unfavorable energy-dependent background is negligibly small in the energy range close to the Fermi level. Thus only the constant background was subtracted from the UPS spectra.

We found that the calculated thermoelectric power of CCO obtained by inserting measured UPS intensity for $N(\varepsilon)$ in Eq. (3) is qualitatively consistent with the measured one in the sense that a large positive thermoelectric power with a positive temperature coefficient was reproduced.[30] Unfortunately, however, the absolute value of the calculated thermoelectric power was only half of the measured ones over a whole temperature range.

We consider the difference between measured and calculated thermoelectric power to be most likely caused by the inappropriate assumption of the energy-independent group velocity. It is obvious from the RPES and UPS spectra that E_F is located at the band edge. In such a case, the group velocity must be strongly energy dependent; it decreases with approaching the band edge and eventually becomes zero at the band edge. Thus an energy dependence of the group velocity is introduced in the present analysis to allow more quantitative discussion on the thermoelectric power.

If there is no significant variation in electronic effective mass m at the energy range in which the calculation is performed, the $\varepsilon-k$ dispersion near the high-energy band edge can be described as

$$\varepsilon=\varepsilon_{max}-\frac{\hbar^2}{2m_x}(k_x-k_{xo})^2-\frac{\hbar^2}{2m_y}(k_y-k_{yo})^2-\frac{\hbar^2}{2m_z}(k_z-k_{zo})^2, \tag{4}$$

where (k_{xo},k_{yo},k_{zo}) represents the wave vector at the highest energy ε_{max} in the band. A smaller electrical resistivity in

the a,b planes than that along the c axis[3,5] allows us to employ the condition of $m_x \ll m_z$ and $m_y \ll m_z$, so that the dispersion along the z direction can be safely ignored. The electronic structure calculated for γ-NCO by LDA-LAPW method[17] indeed shows a less dispersive $\varepsilon - k$ relation along c axis than that in the a,b plane.

Under the assumption of isotropic electronic structure in the a,b plane, the group velocity is calculated as a function of energy by

$$v(\varepsilon) = \sqrt{\frac{2(\varepsilon_{max} - \varepsilon)}{m_x}}. \tag{5}$$

By substituting Eq. (5) into Eq. (1) and assuming the energy-independent relaxation time τ, we obtained the following formula to evaluate the thermoelectric power:

$$S(T) = \frac{1}{eT} \frac{\int_{-\infty}^{\infty} \tau v(\varepsilon)^2 N(\varepsilon)(\varepsilon - \mu) \frac{\partial f(\varepsilon)}{\partial \varepsilon} d\varepsilon}{\int_{-\infty}^{\infty} \tau v(\varepsilon)^2 N(\varepsilon) \frac{\partial f(\varepsilon)}{\partial \varepsilon} d\varepsilon}$$

$$= \frac{1}{eT} \frac{\int_{-\infty}^{\infty} |\varepsilon_{max} - \varepsilon| N(\varepsilon)(\varepsilon - \mu) \frac{\partial f(\varepsilon)}{\partial \varepsilon} d\varepsilon}{\int_{-\infty}^{\infty} |\varepsilon_{max} - \varepsilon| N(\varepsilon) \frac{\partial f(\varepsilon)}{\partial \varepsilon} d\varepsilon}. \tag{6}$$

The effective mass is canceled in Eq. (6) and, hence, all we need to know to calculate $S(T)$ is the density of states $N(\varepsilon)$ over the energy range where $\partial f(\varepsilon)/\partial \varepsilon$ is finite. Thus the angle integrated UPS spectra of the layered cobalt oxides are employed again for $N(\varepsilon)$ in Eq. (6).

The band structure of the γ-NCO calculated by the LDA-LAPW method indicated the presence of three different hole-like Fermi surfaces.[17] Two of them are almost degenerated and are much larger than that of the third one. By ignoring the contribution from the smaller Fermi surface and assuming a doubly degenerated Fermi surface in the Brillouin zone, we can obtain an $\varepsilon - k$ dispersion similar to that in our assumption described above. Note that no states exist from a few hundred meV to $\sim$1.3 eV above E_F in the LDA-LAPW calculation.[17] The contribution of the conduction bands 1.3 eV above E_F can be ignored in the present calculations because of negligibly small $\partial f(\varepsilon)/\partial \varepsilon$ in that energy range.

Figures 7(a1)–7(a3) show UPS spectra of the CCO, BSCO, and γ-NCO measured at 300 K together with those divided by the Fermi-Dirac distribution function (UPS/FD spectra). The calculated thermoelectric power by inserting UPS/FD spectra into Eq. (6) are shown in Figs. 7(b1)–7(b3) together with the measured values. The calculated thermoelectric power shows fairly good consistency with the measured one at a quantitative level, in sharp contrast to the much smaller value calculated with Eq. (3) shown with the dotted line in Fig. 7(b1).

Reliable information about the conduction band can be deduced up to $\sim$0.12 eV ($\approx 3k_BT$) in the UPS/FD spectra. One may wonder that the uncertain density of states in the conduction band above 0.12 eV would have crucial effect in enhancing or reducing the calculated thermoelectric power. In order to know how the conduction band more than 0.1 eV above E_F contributes to the thermoelectric power, we employed three different $N(\varepsilon)$ with different cutoff energies ($E_{cut} \approx 0.12$, 0.14, and 0.17) which correspond to the high-energy band edge, and calculated the thermoelectric power of the BSCO with the deduced $N(\varepsilon)$. The resulting thermoelectric power for each model shows essentially the same absolute value and temperature dependence. This result indicates that the density of states at energies more than 0.1 eV above E_F is of less importance for the evaluation of thermoelectric power, and that our analysis on the basis of precisely determined UPS intensity is reliable. We conclude, therefore, that the large thermoelectric power observed in these layered cobalt oxides can be explained within the framework of the Boltzmann-type electrical conduction mechanism and the electrons in the narrow band with its band edge near E_F.

There still remains minor disagreement between the measured and calculated thermoelectric power. The disagreement probably arose from the assumption about the constant effective mass we used in our present analysis. The $\varepsilon - k$ dispersion calculated from the LDA-LAPW method has less dispersive part near the Γ point just above E_F.[17] We expect that if we could take into account this energy dependence of the electronic effective mass, the thermoelectric power of these layered cobalt oxides evaluated from the experimentally determined electronic structure would more precisely agree with the observed one. Recently, ARPES measurements for $Na_{0.6}CoO_2$ and $Na_{0.5}CoO_2$ were performed and the $\varepsilon - k$ dispersion was revealed.[31,32] A holelike cylindrical Fermi surface centered at the Γ point was indeed observed as we assumed in our analysis. An energy variation from the electronic mass similar to the prediction of the theoretical calculation[17] was also determined.[31] We are now in progress in the evaluation of the thermoelectric power using precisely determined $\varepsilon - k$ dispersion with the ARPES measurement.

Wang *et al.*[16] reported that the spin entropy is likely the source of the large thermoelectric power in $Na_xCo_2O_4$ because a strong magnetic-field dependence of the thermoelectric power, which is not commonly observed in metallic compounds, was clearly observed in their experiment. It sounds a very reasonable interpretation. However, it is also possible to think that if the relaxation time of the conduction electrons is determined by the strong electron correlation and if the system has strong asymmetric electron correlation such as that in the high-T_C superconductors,[33] energy dependence of the quasiparticles' lifetime τ would be affected by the presence of the external magnetic field due to the spiral motion of the quasiparticles. If this is the case, a strong magnetic-field dependence of the thermoelectric power would be observed and the combination of anisotropic electron correlation and anisotropic electronic structure would cause an anisotropic magnetic-field dependence of the thermoelectric power as those reported by Wang *et al.*[16] The role of the energy and momentum dependencies of the relaxation time τ will be revealed through the spectrum-shape analysis of our ARPES measurement now in progress.

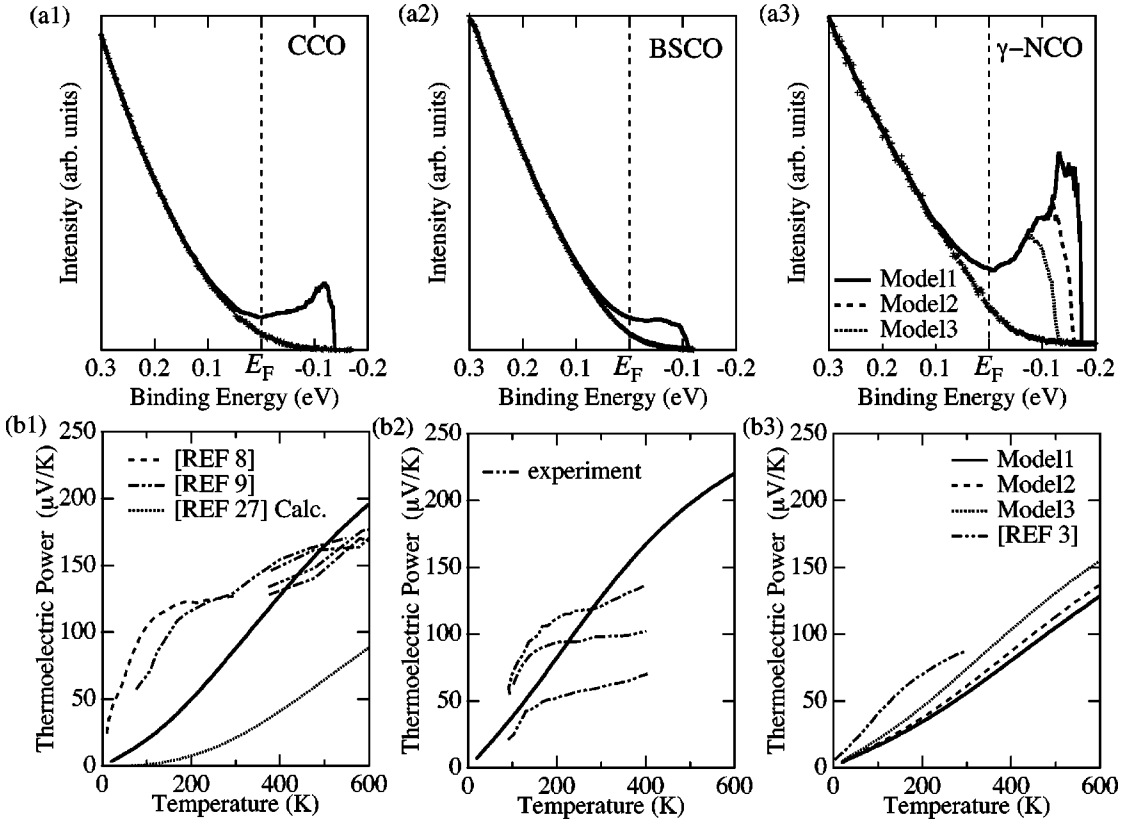

FIG. 7. UPS spectra at 300 K (+) and those divided by the Fermi-Dirac distribution function (UPS/FD spectra; with solid lines) after being smoothed are shown in (a1), (a2), and (a3) for $Ca_3Co_4O_9$ (CCO), $Bi_2Sr_2Co_2O_9$ (BSCO), and γ-$Na_{0.6}CoO_2$ (γ-NCO), respectively. The density of states above E_F is revealed in the UPS/FD spectra. The UPS/FD spectra were used as $N(\varepsilon)$ for the evaluation of thermoelectric power. The deduced thermoelectric power are shown in (b1), (b2), and (b3) with the measured data. Since reliable information about the conduction band can only be deduced up to a few k_BT above E_F in UPS/FD spectra, three different $N(\varepsilon)$ are used for the γ-NCO to calculate its thermoelectric power. No significant difference in the thermoelectric power deduced from these three models was found, and this result strongly supports the reliability of practical use of UPS spectra as $N(\varepsilon)$. Our preliminary analysis with Eq. (2) for the CCO are also superimposed in (b1) with the dotted line. A positive temperature coefficient and large positive value of the thermoelectric power of these cobalt oxides can be better reproduced by analysis using Eq. (6). Strong sample dependence of thermoelectric power was observed in BSCO. It would be related with the localization tendency briefly commented in the Discussion.

V. CONCLUSION

The valence-band structure of the layered cobalt oxides, γ-phase $Na_{0.6}CoO_2$, $Bi_2Sr_2Co_2O_9$, and $Ca_3Co_4O_9$, was determined by combining the bulk-sensitive RPES and high-resolution UPS measurements. The electronic structure near the Fermi level E_F is characterized by a narrow band of less than 2 eV in width and by E_F near its edge. By calculating $S(T)$ from the measured UPS spectrum in the context of the Boltzmann transport equation, we confirmed that this unique electronic structure is solely responsible for the coexistence of the large thermoelectric power and the metallic electrical conduction in these layered cobalt oxides.

ACKNOWLEDGMENTS

One of the authors, T.T., greatly acknowledges Dr. H. Ding, Dr. J. Sugiyama, and Dr. R. Asahi for their valuable comments on this work. The RPES measurements at SPring-8 were performed with the approval of the Japan Synchrotron Radiation Research Institute (JASRI) (Proposal No. 2003A0547-NS1-np).

[1] K. Takeda, H. Sakurai, E. Takayama-Muromachi, F. Izumi, R.A. Dilanian, and T. Sasaki, Nature (London) **422**, 53 (2003).

[2] T. Valla, P.D. Jhonson, Z. Yusof, B. Wells, Q. Li, S.M. Loureiro, R. Cava, M. Mikami, Y. Mori, M. Yoshimura, and T. Sasaki, Nature (London) **417**, 627 (2002).

[3] I. Terasaki, Y. Sasago, and K. Uchinokura, Phys. Rev. B **56**, R12685 (1997).

[4] K. Fujita, T. Mochida, and K. Nakamura, Jpn. J. Appl. Phys., Part 1 **40**, 4644 (2001).

[5] A.C. Masset, C. Michel, A. Maignan, M. Hervieu, O. Toulemonde, F. Studer, B. Raveau, and J. Hejtmanek, Phys. Rev. B **62**, 166 (2000).

[6] R. Funahashi, I. Matsubara, H. Ikuta, T. Takeuchi, U. Mizutani, and S. Sodeoka, Jpn. J. Appl. Phys., Part 2 **39**, L1127 (2000).
[7] R. Funahashi, I. Matsubara, H. Ikuta, T. Takeuchi, and U. Mizutani, Mater. Trans., JIM **42**, 956 (2001).
[8] S. Hébert, S. Lambert, D. Pelloquin, and A. Maignan, Phys. Rev. B **64**, 172101 (2001).
[9] M. Shikano and R. Funahashi, Appl. Phys. Lett. **82**, 1851 (2003).
[10] G. Mahan, B. Sales, and J. Sharp, Phys. Today **50** (3), 42 (1997).
[11] Y. Miyazaki, M. Onoda, T. Oku, M. Kikuchi, Y. Ishii, Y. Ono, Y. Morii, and T. Kajitani, J. Phys. Soc. Jpn. **71**, 495 (2002).
[12] W. Koshibae, K. Tsutsui, and S. Maekawa, Phys. Rev. B **62**, 6869 (2000).
[13] W. Koshibae and S. Maekawa, Phys. Rev. Lett. **87**, 236603 (2001).
[14] A. Maignan, S. Hébert, M. Hervieu, C. Michel, D. Pelloquin, and D. Khomskii, J. Phys.: Condens. Matter **15**, 2711 (2003).
[15] A. Maignan, S. Hébert, L. Pi, D. Pelloquin, C. Martin, C. Michel, M. Hervieu, and B. Raveau, Cryst. Eng. **5**, 365 (2002).
[16] Y. Wang, N.S. Rogado, R.J. Cava, and N.P. Ong, Nature (London) **423**, 425 (2003).
[17] D.J. Singh, Phys. Rev. B **61**, 13 397 (2000).
[18] C. Fouassier, G. Matejka, J.-M. Reau, and P. Hagenmuller, J. Solid State Chem. **6**, 532 (1973).
[19] M. Mikami, M. Yoshimura, Y. Mori, T. Sasaki, R. Funahashi, and I. Matsubara, Jpn. J. Appl. Phys., Part 2 **41**, L777 (2002).
[20] R. Funahashi and M. Shikano, Appl. Phys. Lett. **81**, 1459 (2002).
[21] R. Asahi, J. Sugiyama, and T. Tani, Phys. Rev. B **66**, 155103 (2002).
[22] J. Sugiyama, H. Itahara, T. Tani, J.H. Brewer, and E.J. Ansaldo, Phys. Rev. B **66**, 134413 (2002).
[23] R. Funahashi, I. Matsubara, H. Ikuta, T. Takeuchi, and U. Mizutani, in *Proceedings of the 20th International Conference on Thermoelectrics* edited by J. Zhang (The Institute of Electrical and Electronics Engineers, Danvers, MA, 2001).
[24] E. Abrahams, P.W. Anderson, D.C. Licciardello, and T.V. Ramakrishnan, Phys. Rev. Lett. **42**, 673 (1976).
[25] H.R. Krishnamurthy, C. Jayaprakash, S. Saker, and W. Wenzel, Phys. Rev. Lett. **64**, 950 (1990).
[26] M. Fujita, M. Ishimura, and K. Nakao, J. Phys. Soc. Jpn. **60**, 2831 (1991).
[27] M. Fujita, T. Nakanishi, and K. Machida, Phys. Rev. B **45**, 2190 (1992).
[28] G.C. McIntosh and A.B. Kaiser, Phys. Rev. B **54**, 12 569 (1996).
[29] N.W. Ashcroft and N.D. Mermin, *Solid State Physics* (Saunders College, Orlando, FL, 1976).
[30] T. Takeuchi, T. Kondo, K. Soda, U. Mizutani, R. Funahashi, M. Shikano, S. Tsuda, T. Yokoya, S. Shin, and T. Muro, J. Electron Spectrosc. Relat. Phenom. (to be published).
[31] H.-B. Yang, S.-C. Wang, A.K.P. Sekharan, H. Matsui, S. Souma, T. Sato, T. Takahashi, T. Takeuchi, J.C. Campuzano, R. Jin, B.C. Sales, D. Mandrus, Z. Wang, and H. Ding, cond-mat/0310532 (unpublished).
[32] M.Z. Hasan, Y.-D. Chuang, A.P. Kuprin, Y. Kong, D. Quian, Y.W. Li, B.L. Mesler, Z. Hussain, A.V. Fedrov, R. Kimmerling, E. Rotenberg, K. Rossanagel, H. Koh, M. Rogado, M.L. Foo, and R.J. Cava, cond-mat/0308438 (unpublished).
[33] R. Hlubina, and T.M. Rice, Phys. Rev. B **51**, 9253 (1995); B.P. Stojkovic and D. Pines, Phys. Rev. Lett. **76**, 811 (1996).